



**Combined iron and thyroid hormone protocol suppresses
ischemia-reperfusion injury in rat liver**

Journal:	<i>RSC Advances</i>
Manuscript ID:	RA-ART-12-2014-015863.R1
Article Type:	Paper
Date Submitted by the Author:	04-Mar-2015
Complete List of Authors:	Pedemonte, Juan; University of Chile, Faculty of Medicine, ICBM Vargas, Romina; University of Chile, Faculty of Medicine, ICBM Castillo, Valentina; University of Chile, Faculty of Medicine, ICBM Hodali, Tomas; University of Chile, Faculty of Medicine, ICBM Gutierrez, Sebastian; University of Chile, Faculty of Medicine, ICBM Tapia, Gladys; University of Chile, Faculty of Medicine, ICBM Castillo, Ivan; University of Chile, Faculty of Medicine, ICBM Videla, Luis; University of Chile, Faculty of Medicine, ICBM; University of Chile, Faculty of Medicine, Molecular & Clinical Pharmacology Program, Institute of Biomedical Sciences Fernandez, Virginia; University of Chile, Faculty of Medicine, ICBM

Combined iron and thyroid hormone protocol suppresses ischemia-reperfusion injury in rat liver

J.C. Pedemonte^{1,2}, R. Vargas¹, V. Castillo¹, T. Hodali¹, S. Gutiérrez¹, G Tapia¹ I. Castillo³, L.A. Videla¹ and V. Fernández^{1,*}

¹Program of Molecular and Clinical Pharmacology, Institute of Biomedical Sciences, Faculty of Medicine, University of Chile, Santiago, Chile

²Anesthesiology Division, Faculty of Medicine, Pontifical Catholic University of Chile, Santiago, Chile. ³School of Medicine, Faculty of Medicine, Catholic University of Talca, Chile

Running title: Iron/thyroid hormone liver preconditioning

***Corresponding author:** Virginia Fernández, Molecular and Clinical Pharmacology Program, Institute of Biomedical Sciences, Faculty of Medicine, University of Chile, Independencia 1027, Casilla 70000, Santiago 7, Chile. Tel: +56-2-29786256; Fax: + 56-2-27372783; Email: vfernand@med.uchile.cl

Abstract

Abstract: Liver preconditioning (PC) against ischemia-reperfusion (IR) injury is attained by iron (Fe) or thyroid hormone (T_3) administration. This study was aimed to evaluate the PC effects of a combined Fe plus T_3 protocol, characterized by reduced period of Fe treatment and low T_3 dosage, against ischemia (1 h)-reperfusion (20 h) injury. Male Sprague-Dawley rats were given Fe (two doses of 50 mg/kg at days 0 and 2), T_3 (0.05 mg/kg at day 5), and subjected to sham operation or IR at day 7. At this time, blood and liver samples were taken for analysis of serum aspartate (AST) and alanine (ALT) aminotransferases and hepatic histology, glutathione (GSH), protein carbonyl, and 8-isoprostane contents, protein levels of nuclear factor E2-related factor 2 (Nrf2)(Western blot), nuclear factor- κ B (NF- κ B) DNA binding (ELISA), and mRNA expression of glutamate-cysteine ligase-c (GCLC) and haptoglobin (real-time quantitative PCR). IR enhanced serum AST and ALT levels with drastic changes in liver morphology, significant enhancement in protein carbonyl/GSH ratios and 8-isoprostane content, diminution in nuclear Nrf2 content and in NF- κ B DNA binding, without changes in GCLC and haptoglobin mRNA expression. These IR-induced changes were not modified by individual Fe or T_3 pre-treatment, but suppressed by the combined Fe plus T_3 protocol with increased GCLC and haptoglobin expression. In conclusion, combined Fe plus T_3 protocol suppresses IR liver injury, a novel PC strategy that is related to normalization of oxidative stress status, Nrf2 and NF- κ B activation, and associated GCLC and haptoglobin upregulation.

Keywords: Iron • Thyroid hormone • Liver preconditioning • Ischemia/reperfusion injury • Oxidative stress • Nrf2 • NF- κ B

Introduction

Liver preconditioning (PC) is a protective strategy used against injuring stimuli such as ischemia-reperfusion (IR), which is aimed to attenuate or avoid the onset of the underlying pathogenic mechanisms. Numerous experimental PC protocols have been introduced in the past, in addition to postconditioning and remote conditioning manoeuvres, however, few of them have reached clinical practice.¹⁻³ Among them, pharmacological liver PC involves agents that either interfere with injurious pathways directly or induce a low level of stress triggering cellular defence processes against a subsequent stronger insult.⁴ Early studies by Clavien et al. revealed that mild burst of oxidative stress induced during ischemic PC triggers protection against IR injury.⁵ This was achieved by the use of the model oxidant *tert*-butyl hydroperoxide,⁵ an effect that is mimicked by pro-oxidant conditions developed by *in vivo* doxorubicin⁶ or ozone⁷ administration, hyperbaric oxygen therapy,⁸ and hyperthermia.⁹

In the last decade, our group has successfully undertaken the evaluation of alternate experimental liver PC protocols that might have application in the clinical setting, including thyroid hormone (T₃),¹⁰ iron (Fe),¹¹ or n-3 long-chain polyunsaturated fatty acids.¹² In particular, a single dose of 0.1 mg T₃/kg¹⁰ or six doses of 50 mg Fe-dextran/kg every second day during ten days¹¹ afford protection against liver damage due to the 1 h ischemia-20 h reperfusion protocol in the rat, which underlie the development of transient, moderate oxidative stress.^{13,14} Taking into account that the PC dose of T₃ and/or the period of Fe administration previously used might lead to undesirable effects limiting their clinical application, the present study was aimed to evaluate the

hepatoprotective effects of an alternate protocol reducing both the period of Fe administration and the dose of T₃ against IR injury. For this purpose, liver PC and oxidative stress status were evaluated in groups of rats subjected to either (i) two doses of 50 mg Fe/kg; (ii) a single dose of 0.05 mg T₃/kg; or (iii) the respective combined Fe plus T₃ protocol. The study included assessment of the activation levels of nuclear factor E2-related factor 2 (Nrf2) and nuclear factor-κB (NF-κB), transcription factors which are known to be redox sensitive and to trigger cytoprotective responses,⁴ in relation to the expression of the antioxidant proteins glutamate cysteine ligase-c (GCLC) regulated by Nrf2 and haptoglobin controlled by NF-κB.

Methods

Animal treatments and model of partial hepatic IR injury.

Male Sprague-Dawley rats (Animal facility of the Institute of Biomedical Sciences, Faculty of Medicine, University of Chile) weighing 150-180 g were housed in a humidity and temperature controlled room with 12-h light/dark cycle, and were provided with rat chow and water ad libitum. At time zero (Table 1A) Fe treatment was initiated with two intraperitoneal (ip) doses of 50 mg of Fe–dextran/kg, dissolved in buffered saline, administered at days 0 and 2, and the control group received isovolumetric amounts of saline. At day 5 the animals received, either a single dose of T₃ (0.05 mg/kg) or isovolumetric amounts of 0.1N NaOH (T₃ vehicle) (Table 1A). At Day 7 the animals were anesthetized with Zoletil 50 (tiletamine chlorohydrate 50 mg/kg/zolazepam chlorohydrate 50 mg/kg; Virbac, Carros, France) and subjected to partial liver ischemia by

temporary occlusion of the blood supply to the left and median lobes, by means of a Schwartz clip (FST, Vancouver, BC, Canada) for 1 h, followed by 20 h of reperfusion, as previously described.¹⁵ Control animals were subjected to anesthesia and sham laparotomy, thus comprising eight experimental groups: (a) saline-NaOH-sham, (b) saline-NaOH-IR, (c) Fe-NaOH-sham, (d) Fe-NaOH-IR, (e) saline-T₃-sham, (f) saline-T₃-IR, (g) Fe-T₃-sham, and (h) Fe-T₃-IR (Table 1A). At the end of the reperfusion period, blood samples were obtained by cardiac puncture, for serum aspartate amino transferase (AST) and alanine amino transferase (ALT) assessment. Liver samples were taken from the medial lobes, frozen in liquid nitrogen and stored at -80°C for ELISA (p65 NF-κB and 8-isoprostanes), Western blot (Nrf2), and qPCR (haptoglobin and GCLC) assays. Experimental animal protocols and animal procedures complied with the Guide for the Care and Use of Laboratory Animals (National Academy of Sciences, NIH Publication 86-23, revised 1985) and approved by the Bioethical Committee (Faculty of Medicine, University of Chile, protocol CBA 0381 FMUCH).

Assessment of liver injury and oxidative stress-related parameters.

Serum AST and ALT were measured using specific commercial kits (Valtek Diagnostics, Santiago, Chile) and expressed as international units per liter. Liver morphological assessment was carried out in liver samples fixed in phosphate-buffered formalin, paraffin embedded, stained with hematoxylin–eosin, and evaluated by a pathologist (I.C., double blinded) in order to determine hepatocellular necrosis and the score for liver injury.¹⁶

In anesthetized animals, livers were perfused *in situ* with a cold solution containing 150 mM KCl and 5 mM Tris (pH 7.4) to remove blood, and total reduced glutathione (GSH) equivalents,¹⁷ protein carbonyl, and total protein contents were measured.¹⁸ Non-perfused liver samples were subjected to ELISA assay for the assessment of liver 8-isoprostane content.

ELISA assessment of NF- κ B DNA binding and 8-isoprostanes content.

Nuclear protein extracts from liver samples were prepared using a commercial kit (Nuclear Extraction Kit N° 10009277, Cayman Chemical Company, Ann Arbor, MI, USA), containing protein inhibitors (lyophilized Protease Inhibitor Cocktail). Nuclear extracts were used for p65 NF- κ B DNA binding activity, using a transcription factor assay kit, (Cayman Chemical Co, Ann Arbor, MI, USA), according to manufacturers instructions. Whole liver extracts were used for 8-isoprostanes evaluation (8-isoprostanes ELISA kit, Cayman Chemical Company, Ann Arbor, MI, USA) according to the manufacturer's instructions.

Western blot analysis of nuclear Nrf2.

Nuclear (35 μ g) protein extracts, prepared as already described, were used for western blot analysis of Nrf2 content. This protein was separated on 12% polyacrylamide gels using SDS-PAGE and transferred to nitrocellulose membranes,^{19,20} which were blocked for 1 h at room temperature with TBS containing 5% serum bovine albumin. The blots were washed with TBS containing 0.1% Tween 20 and hybridized with a rabbit polyclonal antibody for

Nrf2 (Cell Signalling Technology Inc., MA, USA). In all determinations, rabbit monoclonal antibody for rat lamin A/C (Cell Signalling Technology Inc., MA, USA) was used as internal control for nuclear fractions, whereas rabbit monoclonal antibody for cytosolic β -actin (Cell Signalling Technology, Inc., MA, USA) controlled the purity of the nuclear fractions. After extensive washing, the antigen–antibody complexes were detected using horseradish peroxidase goat anti-rabbit IgG and a SuperSignal West Pico Chemiluminescence kit detection system (Pierce, Rockford, IL). Bands were quantified by densitometry using a Gel Documentation System, Biosens SC-750 (Shanghai Bio-Tech Co., Ltd., China). Results were normalized with respect to Lamin A/C.

Real-time quantitative PCR for haptoglobin and GCLC.

Total RNA was extracted from 30 mg of liver with a Qiagen RNeasy kit (Qiagen Sciences, Maryland, USA) according to the manufacturer's instructions. Complementary DNA (cDNA) was prepared using reverse transcriptase ThermoScript RT-PCR System, (Life Technologies Corporation, Carlsbad, California, USA) according to the manufacturer's instructions. Forward and reverse primers were designed for the genes rat haptoglobin, GCLC, Rps23, and β -actin (Table 1B). Primers were optimized to yield 95%–100% reaction efficiency, and PCR products were run on agarose gels to verify the correct amplification length. Melt curve analyses verified the formation of a single desired PCR product in each PCR reaction. The expression level of each sample was normalized against Rps23 or β -actin (data not shown) as internal controls. The relative expression level was calculated using the comparative C_T

method ($\Delta\Delta C_T$) and values were normalized to Rps23 level. Real-time quantitative PCR was carried out in a Stratagene Mx3005P (Agilent Technologies, California, USA) using Brilliant II SYBR Green QPCR Master Mix (Agilent Technologies, California, USA) following the manufacturer's protocols.

Statistics

Values shown represent the mean \pm SEM for the number of separate experiments indicated. Two-way ANOVA and the Newman–Keuls' test assessed the statistical significance of differences between mean values (a *P* value of < 0.05 was considered significant). Net effects of IR were obtained by subtracting average values in sham-operated groups from individual values in IR groups, namely, $b - a$ (untreated control), $d - c$ (Fe pre-treatment), $f - e$ (T_3 pre-treatment), and $h - g$ (combined Fe plus T_3 protocol)(see Table 1A). Associations between variables were computed using the Pearson correlation coefficient (GraphPad Prism 2.0 software GraphPad Software, San Diego, CA, USA).

Results

We first analysed the hepatic oxidative stress status in animals subjected to either the Fe protocol alone for up to 72 h or the T_3 protocol alone for up to 48 h (Table 1A), without surgical procedures. Liver protein carbonylation was significantly increased at 24 h post-Fe treatment (Fig. 1A) whereas those of GSH diminished at 24 and 48 h (Fig. 1B), thus enhancing ($P < 0.05$) the oxidative

stress status indicative parameter protein carbonyl/GSH ratio at 24 h (Fig. 1C), parameters that were normalised 72 h post-Fe. T₃ administration exhibited similar changes ($P<0.05$) at 24 h post-T₃, including liver protein carbonyl enhancement (Fig. 1D), GSH depletion (Fig. 1E), and increment in the protein carbonyl/GSH ratio (Fig. 1F), which were normalised at 48 h.

The oxidative stress level of the liver after IR in rats previously subjected to the combined Fe plus T₃ protocol and the respective control groups (Table 1A) is presented in Fig. 2, with net changes shown in the insets. As can be observed, IR increased the content of hepatic protein carbonyls by 231% (Fig. 2A and inset) and decreased that of GSH by 38% (Fig. 2B and inset), leading to 456% enhancement in the protein carbonyl/GSH ratio (Fig. 2C and inset), with concomitant 102% higher 8-isoprostane levels (Fig. 2D and inset) over the respective sham operated groups. Following the administration of Fe alone or T₃ alone, IR-induced changes in these parameters were not completely suppressed, as occurred after the combined Fe plus T₃ protocol (Fig. 2 A, B, C, D, and insets). Under these conditions, protein carbonyl/GSH ratios were significantly correlated with 8-isoprostane level ($r=0.85$; $P<0.01$) and inversely associated with GSH contents ($r=-0.76$; $P<0.02$). Furthermore, the IR-induced ([protein carbonyl/GSH]_{Fe + T₃}) ratio normalised by the respective control value ratio was 5.47 ± 0.74 ($n=5$) (from Fig. 2C), which was significantly higher ($P<0.05$) than the maximal values achieved by the separate pre-treatment with Fe ([protein carbonyl/GSH]_{Fe} = 3.01 ± 0.42 ($n=5$)) or T₃ ([protein carbonyl/GSH]_{T₃} = 2.22 ± 0.27 ($n=4$)) without IR (from Fig. 1, C and F, respectively).

We next studied the influence of Fe, T₃, and combined Fe plus T₃ protocols (Table 1A) on parameters associated with IR-induced liver injury (Fig. 3). IR achieved extensive liver injury as evidenced by (i) significant 4.4-fold and 3.4-fold increases in serum AST (Fig. 3, A and B), and ALT (Fig. 3, C and D) over sham-operated animals, respectively, and (ii) substantial distortion of liver architecture with extensive areas of hepatocyte necrosis and infiltration by polymorphonuclear leukocytes (Fig. 3E (b)) resulting in high necrosis (Fig. 3F) and inflammation (Fig. 3G) scores, compared to vehicle-controls showing normal liver morphology (Fig. 3E (a)). Although IR-induced AST and ALT levels in serum were significantly lower in rats subjected to individual Fe and T₃ protocols than those elicited by IR in untreated animals (Fig. 3, A, B, C, and D), distorted liver architecture (Fig. 3E(d)) with high necrosis and inflammation scores (Fig. 3, F and G) were observed after IR in Fe pre-treated rats, whereas animals pre-treated with T₃ showed conserved liver architecture, focal necrosis (Figs. 3E(f) and 3F), and inflammatory response (Fig. 3G), compared to the respective sham-operated controls (Fig. 3, (c) and (e)). On the contrary, combined Fe plus T₃ protocol suppressed liver IR injury, as shown by normalization of AST and ALT levels in serum (Fig. 3, A, B, C, and D), the presence of normal liver architecture (Fig. 3E(h)), and absence of necrosis (Fig. 3F) and inflammation (Fig. 3G), similar to the respective Fe-T₃-sham operated control (Fig. 3(g)). Fibrosis was not observed in any of the experimental groups studied. These changes are strengthened by the significant correlations found between serum AST and ALT levels with the respective necrosis scores ($r=0.90$, $P<0.002$ and $r=0.80$, $P<0.01$, respectively) and inflammation scores ($r=0.98$, $P<0.0001$ and $r=0.93$, $P<0.0005$, respectively).

We finally tested whether combined Fe plus T₃ protocol resulted in changes in Nrf2 and NF-κB signaling affording liver protection against IR injury (Fig. 4). In this respect, liver levels of nuclear Nrf2 were significantly reduced by IR in untreated animals and in rats given Fe, unaltered in those given T₃ alone, and enhanced by the combined Fe plus T₃ protocol (Fig. 4A). Images shown in Fig. 4A correspond to two different gels, comprising samples from groups a to d and e to h, respectively, with average values shown in the columns below. Together, these data resulted in significant diminution in the nuclear Nrf2 levels by IR in the liver of untreated rats and in animals subjected to individual Fe or T₃ protocols, whereas combined Fe plus T₃ administration elicited a substantial enhancement (Fig. 4B)(*P*<0.05). In addition, liver GCLC mRNA expression controlled by Nrf2 was not altered by IR in untreated animals and in those given Fe or T₃ over the respective controls, whereas combined Fe plus T₃ protocol achieved a significant enhancement (Fig. 4, C and D). In addition to Nrf2 signaling, IR resulted in significant reductions in liver NF-κB p65 DNA binding in untreated animals and in those pre-treated with Fe or T₃ alone, except for that observed in rats subjected to the combined Fe plus T₃ protocol (Fig. 4E). In this latter group, recovery of NF-κB p65 DNA binding (Fig. 4, E and G) was paralleled by a significant increase in the mRNA expression of the gene for haptoglobin (Fig. 4, F and G) controlled by NF-κB. In agreement with these findings, Nrf2 and NF-κB activation were significantly correlated with the mRNA expression of GCLC (*r*=0.94; *P*<0.03) and that of haptoglobin (*r*=0.99; *P*<0.0002), respectively.

Discussion

Oxidative stress develops upon occurrence of an imbalance between pro-oxidant and antioxidant species in favour of the pro-oxidants. The phenomenon has hormetic connotations, considering that at low levels it stimulates protective mechanisms leading to biologically beneficial effects, whereas responses at high levels are potentially harmful.^{5,21} In agreement with this contention, development of low, transient levels of the hepatic oxidative stress-related protein carbonyl/GSH ratio by individual Fe or T₃ administration afforded PC effects only when combined, whereas high protein carbonyl/GSH ratios achieved by IR attained severe liver injury. In the latter case, the drastic development of oxidative stress by IR is associated with significant loss of Nrf2 and NF-κB signaling, with the respective GCLC and haptoglobin mRNA levels being set at basal values. These findings point to lack of adequate antioxidant protection following IR, a condition that is reinforced by the failure in the adaptation of hepatic inducible nitric oxide synthase expression and activity.²²

Low, transient oxidative stress in the liver induced by separate Fe and T₃ administration lacking PC effects, achieved full protection against IR injury when Fe treatment was followed by a single dose of T₃. Combined Fe plus T₃-induced liver PC is related to enhancement in hepatic nuclear protein Nrf2 levels, with concomitant upregulation of GCLC mRNA expression controlled by Nrf2, parameters that are significantly correlated. The increase in the protein content of Nrf2 in the nucleus over basal values is considered an activating step, taking into account that pro-oxidant conditions promote the inactivation of the Nrf2 negative regulator Keap1 in the cytosol, favouring Nrf2 nuclear translocation and target gene transcription.²³ GCLC constitutes the rate-limiting enzyme in the biosynthesis of the main hydrosoluble antioxidant GSH, whose induction by

Fe plus T₃ protocol promotes liver GSH recovery after depletion by IR (Fig. 2B), whereas lack of GCLC in Nrf2^(-/-) mice depletes renal GSH stores upon treatment with ferric nitrilotriacetate.²⁴ Besides GCLC, promotion of a high antioxidant status in the liver by the combined Fe plus T₃ protocol may be contributed by mechanisms triggered by either Fe or T₃ individually. These include Nrf2-dependent upregulation of (i) catalase, glutathione-S-transferase (GST), and heme-oxygenase-1 (HO-1) induced by Fe in mice;²⁵ and (ii) thioredoxin,²⁶ GST Ya and Yp,²⁷ and HO-1 elicited by T₃ in rats.²⁸ Other than antioxidant protein induction, T₃-induced Nrf2 activation is associated with upregulation of the expression of detoxification enzymes (NADPH-quinone oxidoreductase-1 and microsomal epoxide hydrolase) and drug transport proteins (multidrug resistance-associated proteins 2 and 3),²⁷ which may afford cytoprotection underlying liver PC by the Fe plus T₃ protocol injury mediated by ROS or by chemical toxicity. The latter aspect, however, remains to be studied. Interestingly, Nrf2 activation regulates Fe metabolism through upregulation of ferroportin-1 mRNA expression, the only Fe exporter in mammals,²⁹ whereas Fe overload induces ferritin synthesis, a protein highly effective in sequestering large amounts of Fe.¹¹ These findings point to significant ferroportin-1-induced Fe reutilization and ferritin-dependent Fe quelation in the liver, which may limit excessive cellular ROS production and toxicity, thus allowing the expansion of the hepatic labile Fe pool associated with hepatoprotection.¹¹ Moreover, potential crosstalk between Nrf2 and NF-κB signaling pathways may lead to anti-inflammatory responses induced by Fe plus T₃ PC. These could be achieved either by (i) the higher antioxidant status induced by Nrf2 activation that limits ROS levels³⁰ and the redox activation of NF-κB;³⁰ and/or (ii) inhibition

of NF- κ B transcriptional activation that is mediated by the abrogation of inhibitor of NF- κ B kinase (IKK) phosphorylation, which in turn limits NF- κ B nuclear translocation otherwise triggering pro-inflammatory signaling.³¹

In addition to Nrf2 signaling, combined Fe plus T₃ administration inducing liver PC against IR injury is also associated with recovery of NF- κ B activation towards basal levels, a finding that significantly correlates with haptoglobin mRNA expression, a type-I acute-phase response protein controlled by NF- κ B. The main function of haptoglobin is the binding of free haemoglobin to prevent damage due to ROS production by free haemoglobin, an antioxidant function that is mediated by prevention of Fe release from haemoglobin upon its binding.³² Furthermore, haptoglobin exhibits anti-inflammatory properties upon suppression of TNF- α secretion by macrophages and promotion of anti-inflammatory cytokine secretion due to haptoglobin-haemoglobin complex binding to CD163 on macrophages.³³ Hepatoprotection achieved by the Fe plus T₃ protocol may include T₃-induced, NF- κ B-dependent upregulation of other important antioxidant components such as manganese superoxide dismutase and inducible nitric oxide synthase, besides the anti-apoptotic protein Bcl2.⁴ It is important to point that T₃ also causes the redox activation of transcription factor activating protein 1 (AP-1) and signal transducer and activator of transcription 3 (STAT3) that, in concert with NF- κ B, trigger cell proliferation, an adaptive response that may compensate for liver cell loss associated with IR-induced hepatocellular necrosis.^{10,22}

In conclusion, combined Fe plus T₃ comprising reduced Fe and T₃ dosages compared to those previously reported in separate trials,^{10,11} abrogates IR liver injury. This is evidenced by suppression of serum AST and ALT level

enhancement, distorted liver architecture, and high necrosis and inflammation scores induced by IR. The combined Fe plus T₃ manoeuvre studied represents a novel PC strategy whose efficacy, compared to the treatments performed independently, is related to the attainment of significant antioxidant and anti-inflammatory responses underlying normalization of Nrf2 and NF-κB signaling depressed by IR. Interestingly, the Fe component of the combined protocol used amounting to 2 doses of 50 mg Fe/kg on alternate days is in the lower range of that employed in the treatment of human anemia, consisting in 100-125 mg Fe/kg given 1-3 times/week for 4-12 weeks, which represents a well tolerated therapeutic strategy.^{34,35} Besides, the T₃ component of the combined protocol employed (0.05 mg/kg; total dose of 10 µg T₃ in a 0.2 Kg body weight rat) is within the range of that utilized in the procurement of abdominal organs from brain-dead donors (total doses of 4 to 42 µg T₃ in a 70 kg man given as an intravenous bolus repeated hourly twice),^{36,37} which enhances the number of organs being functionally acceptable and the early and intermediate graft survival time.³⁸ The beneficial actions of thyroid hormones are also evidenced by (i) the protective effects against IR injury observed not only in the liver,^{10,12,22,39} but also in the heart,⁴⁰ kidney,⁴¹ and brain⁴² of experimental animals; (ii) the critical role in the recovery and repair of tissues subjected to other types of experimental injury, such as mechanical damage, hyperoxia injury, serum starvation, chemotherapy-induced toxicity, or wound;⁴³ and (iii) the improvement induced by thyroxin in mental, motor, and neurological outcomes in infants < 28 weeks' gestation, which exhibit lower plasma thyroid hormone levels than in term-born infants.⁴⁴ Accordingly, in the scenario of mild, transient oxidative stress development associated with transcriptional activation of

protective genes affording liver PC, the Fe plus T₃ protocol studied warrants further investigation in experimental animals and humans, to support its application in preventing IR injury during liver surgery and liver transplantation using reduced-size grafts from living donors.

Acknowledgements

This study was supported by grant 1110006 from National Fund for Scientific & Technological Development (FONDECYT) (to V.F.), Santiago, Chile.

References

1. R. Bahde R and H.U. Spiegel. Hepatic ischaemia-reperfusion injury from bench to bedside. *Brit. J. Surg.* 2010, **97**, 1461-1475.
2. N. Selzner M. Boehnert, M. Selzner. Preconditioning, postconditioning, and remote conditioning in solid organ transplantation: basic mechanisms and translational applications. *Transp. Rev.* 2012, **26**, 115-124.
3. D. Papapoulos, T. Siempis, E. Theodoraki, G. Tsoulfas. Hepatic ischemia and reperfusion injury and trauma: current concepts. *Arch. Trauma Res.* 2013, **2**, 63-70.
4. V. Fernández, G. Tapia, L.A. Videla. Recent advances in liver preconditioning: thyroid hormone, n-3 long-chain polyunsaturated fatty acids and iron. *World J. Hepatol.* 2012, **4**, 119-128.
5. H.A. Rüdiger, R. Graf, P.A. Clavien. Sub-lethal oxidative stress triggers the protective effects of ischemic preconditioning in the mouse liver. *J. Hepatol.* 2003, **39**, 972-977.
6. K. Ito, H. Ozasa, K. Sanada, S. Horikawa. Doxorubicin preconditioning: a protection against rat hepatic ischemia-reperfusion injury. *Hepatology* 2000, **31**, 416-419.
7. H.H. Ajamieh, S. Menéndez, G. Martínez-Sánchez, E. Candelario-Jalil, A. Giuliani, O.S. Fernández.. Effects of ozone oxidative preconditioning on nitric oxide generation and cellular redox balance in a rat model of hepatic ischaemia-reperfusion. *Liver Int.* 2004, **24**, 55-62.

8. S-Y Yu, J-H Chiu, S-D Yang, C-C Hsieh, P-J Chen, W-Y Lui, C-W Wu. Preconditioned hyperbaric oxygenation protects the liver against ischemia-reperfusion injury in rats. *J, Surg, Res*, 2005, **128**, 28-36.
9. H. Terajima, G. Enders, A. Thiaener, C. Hammer, T. Kondo, J. Thiery, Y. Yamamoto, Y. Yamaoka, K. Messmer. Impact of hyperthermic preconditioning on postischemic hepatic microcirculatory disturbances in an isolated perfusion model of the rat liver. *Hepatology* 2000, **31**, 407-415.
10. V. Fernández, I. Castillo, G. Tapia, P. Romanque, S. Uribe-Echevarría, M. Uribe, D. Cartier-Ugarte, G. Santander, M.T. Vial, L.A. Videla. Thyroid hormone preconditioning: protection against ischemia-reperfusion liver injury in the rat. *Hepatology* 2007, **45**, 170-177.
11. M. Galleano, G. Tapia, S. Puntarulo, P. Varela, L.A. Videla, V. Fernández. Liver preconditioning induced by iron in a rat model of ischemia/reperfusion. *Life Sci*. 2011, **89**, 221-228.
12. J. Zúñiga, F. Venegas, M. Villarreal, D. Núñez, M. Chandía, R. Valenzuela, G. Tapia, P. Varela, L.A. Videla, V. Fernández. Protection against in vivo liver ischemia-reperfusion injury by n-3 long-chain polyunsaturated fatty acids in the rat. *Free Radic. Res*. 2010, **44**, 854-863.
13. V. Fernandez, G. Tapia, P. Varela, L. Gaete, G. Vera, C. Mora, M.T. Vial, L.A. Videla. Causal role of oxidative stress in liver preconditioning by thyroid hormone in rats. *Free Radic. Biol. Med*. 2008, **44**: 1724-31.
14. V. Fernández, R. Vargas, V. Castillo, N. Cádiz, D. Bastías, S. Román, G. Tapia, L.A. Videla. Reestablishment of ischemia-reperfusion liver injury by N-

acetylcysteine administration prior to a preconditioning iron protocol. *Scientific World J.* 2013, 2013:607285. DOI: 10.1155/2013/607285.

15. B. Gonzalez-Flecha, J.C. Cutrin, A. Boveris. Time course and mechanism of oxidative stress and tissue damage in rat liver subjected to in vivo ischemia–reperfusion. *J Clin. Invest.* 1993, **91**, 456–464.

16. S. Korourian, R. Hakkak M.J. S.R: Ronis Shelnutt, J. Waldron, M. Ingelman-Sundberg, T.M. Badger. Diet and risk of ethanol-induced hepatotoxicity: carbohydrate-fat relationships in rats. *Toxicol. Sci.* 1999, **47**, 110-117.

17. F. Tietze. Enzymic method for quantitative determination of nanogram amounts of total and oxidized glutathione: applications to mammalian blood and other tissues. *Anal. Biochem.* 1967, **27**, 502-522.

18. A.Z. Reznick, L. Packer. Oxidative damage to proteins: spectrophotometric method for carbonyl assay. *Methods Enzymol.* 1994, **233**, 357–363.

19. U.K. Laemmli. Cleavage of structural proteins during assembly of the head of bacteriophage T4. *Nature* 1970, **227**, 680–685.

20. H. Towbin, T. Staehelin, J. Gordon. Electrophoretic transfer of proteins from polyacrylamide gels to nitrocellulose sheets: procedure and some applications. *Proc. Natl. Acad. Sci. USA* 1979, **76**, 4350–4354.

21. L.A. Videla. Hormetic responses of thyroid hormone calorigenesis in the liver: association with oxidative stress. *IUBMB Life* 2010, **62**, 460-466.

22. V. Fernández, G. Tapia, P. Varela, P. Cornejo, L.A. Videla. Upregulation of liver inducible nitric oxide synthase following thyroid hormone preconditioning: suppression by N-acetylcysteine. *Biol. Res.* 2009, **42**, 487-495.
23. D.D. Zhang. Mechanistic studies of the Nrf2-Keap1 signaling pathway. *Drug Metab. Rev.* 2006, **38**, 769-789.
24. K. Kanki, T. Umemura, Y. Kitamura, Y. Ishii, Y. Kuroiwa, Y. Kodama, K. Itoh, M. Yamamoto, A. Nishikawa, M. Hirose. A possible role of Nrf2 in prevention of renal oxidative damage by ferric nitrilotriacetate. *Toxicol. Pathol.* 2008, **36**, 353-361.
25. K. Moriya, H. Miyoshi, S. Shinzawa, T. Tsutsumi, H. Fujie, K. Goto, Y. Shintani, H. Yotsuyanagi, K. Koike. Hepatitis C virus core protein compromises iron-induced activation of antioxidants in mice and HepG2 cells. *J. Med. Virol.* 2010, **82**, 776-792.
26. P. Romanque, P. Cornejo, S. Valdés, L.A. Videla. Thyroid hormone administration induces rat liver Nrf2 activation: suppression by N-acetylcysteine pretreatment. *Thyroid* 2011, **21**, 655-662.
27. P. Cornejo, R. Vargas, L.A. Videla. Nrf2-regulated phase-II detoxification enzymes and phase-III transporters are induced by thyroid hormone in rat liver. *BioFactors* 2013, **39**, 514-521.
28. L.A. Videla, P. Cornejo, I. Castillo, P. Romanque. Thyroid hormone-induced regulatory interrelations in rat liver Nrf2-Keap1 signaling related to antioxidant enzyme expression. In: Berhardt LB, ed. *Advances in Medicine and Biology*. Volume 55. New York: Nova Science Publishers, 2012, 179-191.

29. N. Harada, M. Kanayama, A. Maruyama, A. Yoshida, K. Tazumi, T. Hosoya, J. Mimura, T. Toki, J.M. Maher, M. Yamamoto, K. Itoh. Nrf2 regulates ferroportin 1-mediated iron efflux and counteracts lipopolysaccharide-induced ferroportin 1 mRNA suppression in macrophages. *Arch. Biochem. Biophys.* 2011, **508**, 101-109.
30. S. Singh, S. Vrishni, B.K. Singh, I. Rahman, P. Kakkar. Nrf2-ARE stress response mechanism: a control point in oxidative stress-mediated dysfunctions and chronic inflammatory diseases. *Free Radic. Res.* 2010, **44**, 1267-1288.
31. C. Xu, G. Shen, C. Chen, C. G elinas, A.N.T. Kong. Suppression of NF- B and NF- B-regulated gene expression by sulforaphane and PEITC through I B , IKK pathway in human prostate cancer PC-3 cells. *Oncogene* 2005. **24**, 4486-4495.
32. G. Galicia, W. Maes, B.A. Verbinnen, D. Kasran, D. Bullens, M. Arredouani, J.L. Ceuppens. Haptoglobin deficiency facilitates the development of autoimmune inflammation. *Eur. J. Immunol.* 2009, **39**, 3404-3412.
33. M. Nielsen, S.K. Moestrup. Receptor-targeting of hemoglobin mediated by the haptoglobins: roles beyond heme scavenging. *Blood* 2009, **156**, 764-771.
34. S.B. Silverstein, G.M. Rodgers. Parenteral iron therapy options. *Am. J. Hematol.* 2004, **76**, 74-78.
35. U.D. Bayraktar, S. Bayraktar. Treatment of iron deficiency anemia associated with gastrointestinal tract diseases. *World J. Gastroenterol.* 2010, **16**, 2720-2725.

36. D. Novitzky, D.K. Cooper, J.S. Chaffin, A.E. Greerm L.E. DeBault, N. Zuhdi. Improved cardiac allograft function following triiodothyronine therapy to both donor and recipient. *Transplantation* 1990, **49**, 311-316.
37. V. Jeevanandam, B. Todd, T. Regillo, S. Hellman, C. Eldridge, J. McClurken. Reversal of donor myocardial dysfunction by triiodothyronine replacement therapy. *J. Heart Lung Transpl.* 1994, **13**, 685-687.
38. D.C.K. Cooper, D. Novitzky, W.N. Wicomb, M. Basker, J.D. Rosendale, M. Kauffman. A review of studies relating thyroid hormone therapy in brain-dead organ donors. *Front. Biosci.* 2009, **14**, 3750-3770.
39. A. Taki-Eldin, L. Zhou, H.Y. Xie, K.J. Chen, D. Yu, Y. He, S.S. Zheng. Triiodothyronine attenuates hepatic ischemia/reperfusion injury in a partial hepatectomy model through inhibition of proinflammatory cytokines, transcription factors, and adhesion molecules. *J. Surg. Res.* 2012, **178**, 646-656.
40. C.I. Pantos, V.A. Malliopoulou, I.S. Mourouzis, E.P. Karamanoli, I.A. Paizis, N. Steimberg, D.D. Varonos, D.V. Cokkinos. Long-term thyroxin administration protects the heart in a pattern similar to ischemic preconditioning. *Thyroid* 2002, **12**, 325-329.
41. S.M. Kim, S.W. Kim, Y.J. Jung, S.I. Min, S.K. Min, S.J. Kim, J. Ha. Preconditioning with thyroid hormone (3,5,3-triiodothyronine) prevents renal ischemia-reperfusion injury in mice. *Surgery* 2014, **155**, 554-561.

42. T. Genovese, D. Impellizzeri, A. Ahmad, C. Cornelius, M. Campolo, S. Cuzzocrea, E. Esposito. Post-ischemic thyroid hormone treatment in a rat model of acute stroke. *Brain Res.* 2013, **1513**, 92-102.
43. I. Mourouzis, E. Politi, C. Pantos. Thyroid hormone and tissue repair: new tricks for an old hormone? *J. Thyroid. Res.* 2013, Article ID 312104. DOI:10.1155/2013/312104.
44. A.G. Van Wassenaer, J.H. Kok. Trials with thyroid hormone in preterm infants: clinical and neurodevelopmental effects. *Semin. Perinatol.* 2008, **32**, 423-430.

Figure legends

Figure 1 Rat liver protein carbonyl and GSH contents after Fe or T₃ administration without surgical procedures. (A) Protein carbonyls, (B) GSH, and (C) protein carbonyl/GSH ratios after Fe treatment. (D) Protein carbonyls, (E) GSH, and (F) protein carbonyl/GSH ratios after T₃ administration. Data shown are means ± SEM for 3-10 animals per group. Statistical significance (one-way ANOVA and the Newman-Keuls' test) is indicated by the letters identifying each group.

Figure 2 Rat liver protein carbonyl, GSH, and 8-isoprostane contents after treatment with combined Fe plus T₃ protocol and subjected to IR. The experimental design is shown in Table 1A. (A) Protein carbonyls, (B) GSH, (C) protein carbonyl/GSH ratios, and (D) 8-isoprostanes. Insets to (A), (B), (C), and (D) correspond to net changes calculated as described in Materials and methods. Data shown are means ± SEM for 3-15 animals per group. Statistical significance (one-way ANOVA and the Newman-Keuls' test) is indicated by the letters identifying each group.

Figure 3 Parameters related to liver injury in rats subjected to combined Fe plus T₃ treatment followed by IR. The experimental design is shown in Table 1A. (A) Serum AST, (B) net changes in AST, (C) serum ALT, (D) net changes in ALT, (E) liver histology (hematoxylin-eosin; magnification x 100), (F) liver necrosis score, and (G) liver inflammation score. Net changes shown in (B) and (D) were calculated as described in Materials and methods. Data shown are means ± SEM for 3-8 animals per group. Statistical significance (one-way

ANOVA and the Newman-Keuls' test) is indicated by the letters identifying each group.

Figure 4 Rat liver Nrf2 protein expression, GCLC mRNA expression, NF- κ B p65 DNA binding, and haptoglobin mRNA levels after treatment with combined Fe plus T₃ protocol and subjected to IR. The experimental design is shown in Table 1A. (A) Nuclear Nrf2 (68 kDa), Lamin A/C (70 kDa), and β -Actin (42 kDa), (B) net changes in nuclear Nrf2, (C) GCLC, (D) net changes in GCLC, (E) NF- κ B DNA binding, (F) haptoglobin, and (G) net changes in NF- κ B DNA binding and haptoglobin mRNA expression. Net changes shown in (B), (D), and (G) were calculated as described in Materials and methods. Specific primer pairs for quantitative real-time PCR are listed in Table 1B. Data shown are means \pm SEM for 3-10 animals per group. Statistical significance (one-way ANOVA and the Newman-Keuls' test) is indicated by the letters identifying each group.

Table 1 Experimental design (A) and primer sequence for qRT-PCR (B)

A. Groups	Treatments			Surgeries	
A	Saline	Saline	NaOH	Sham	-
B	Saline	Saline	NaOH	Ischemia	Reperfusion
C	Fe (50 mg/kg)	Fe (50 mg/kg)	NaOH	Sham	-
D	Fe (50 mg/kg)	Fe (50 mg/kg)	NaOH	Ischemia	Reperfusion
E	Saline	Saline	T ₃ (0.05 mg/kg)	Sham	-
F	Saline	Saline	T ₃ (0.05 mg/kg)	Ischemia	Reperfusion
G	Fe (50 mg/kg)	Fe (50 mg/kg)	T ₃ (0.05 mg/kg)	Sham	-
H	Fe (50 mg/kg)	Fe (50 mg/kg)	T ₃ (0.05 mg/kg)	Ischemia	Reperfusion
Time (h)	0	48	72	120	121→141



Sampling

B. mRNA	Forward primer (5'→3')	Reverse primer (5'→3')
Haptoglobin	gaa agg cgc tgt aag tcc tg	gga ccc agt cct tca gat ca
GCLC	ggg aac gaa ggc gtg ttt cct	gtc gac ttc cat gtt ttc aag gt
Rps23	gta ggg gtt gaa gcc aaa ca	cac ctt aaa gcg gac tcc ag
β-actin	agc cat gta cgt agc cat cc	ctc tca gct gtg gtg aa

Fe, iron; GCLC, glutamate-cysteine ligase catalytic subunit; Rps23, ribosomal protein s23

Figure 1

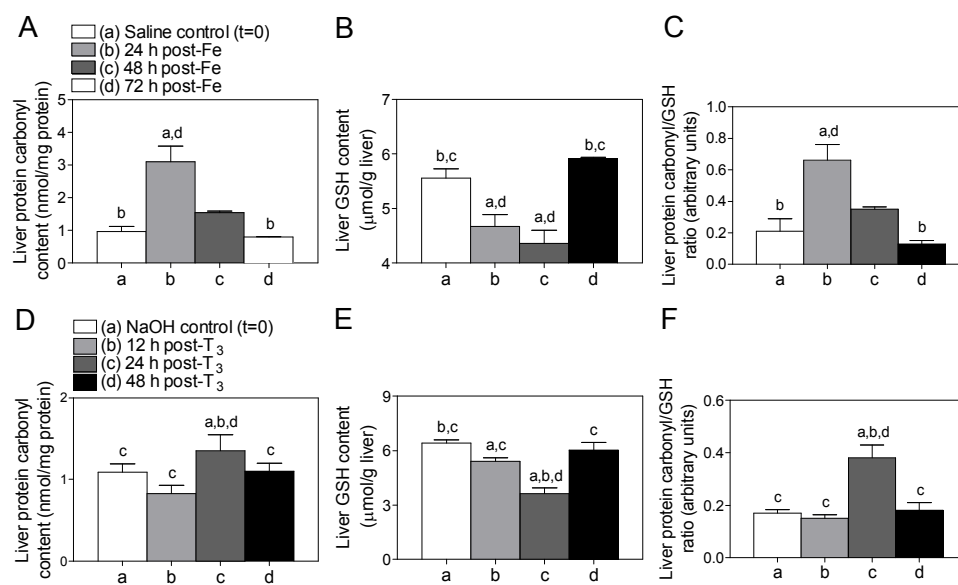


Figure 2

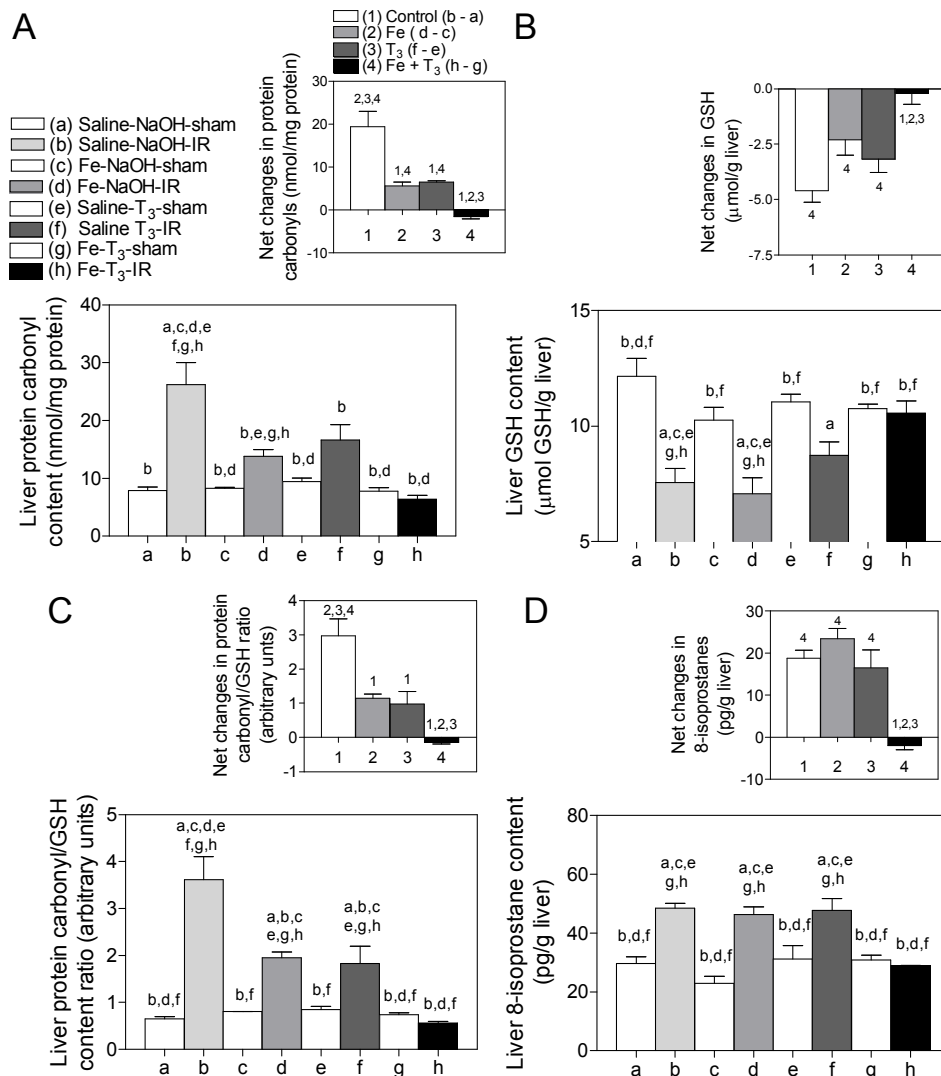


Figure 3

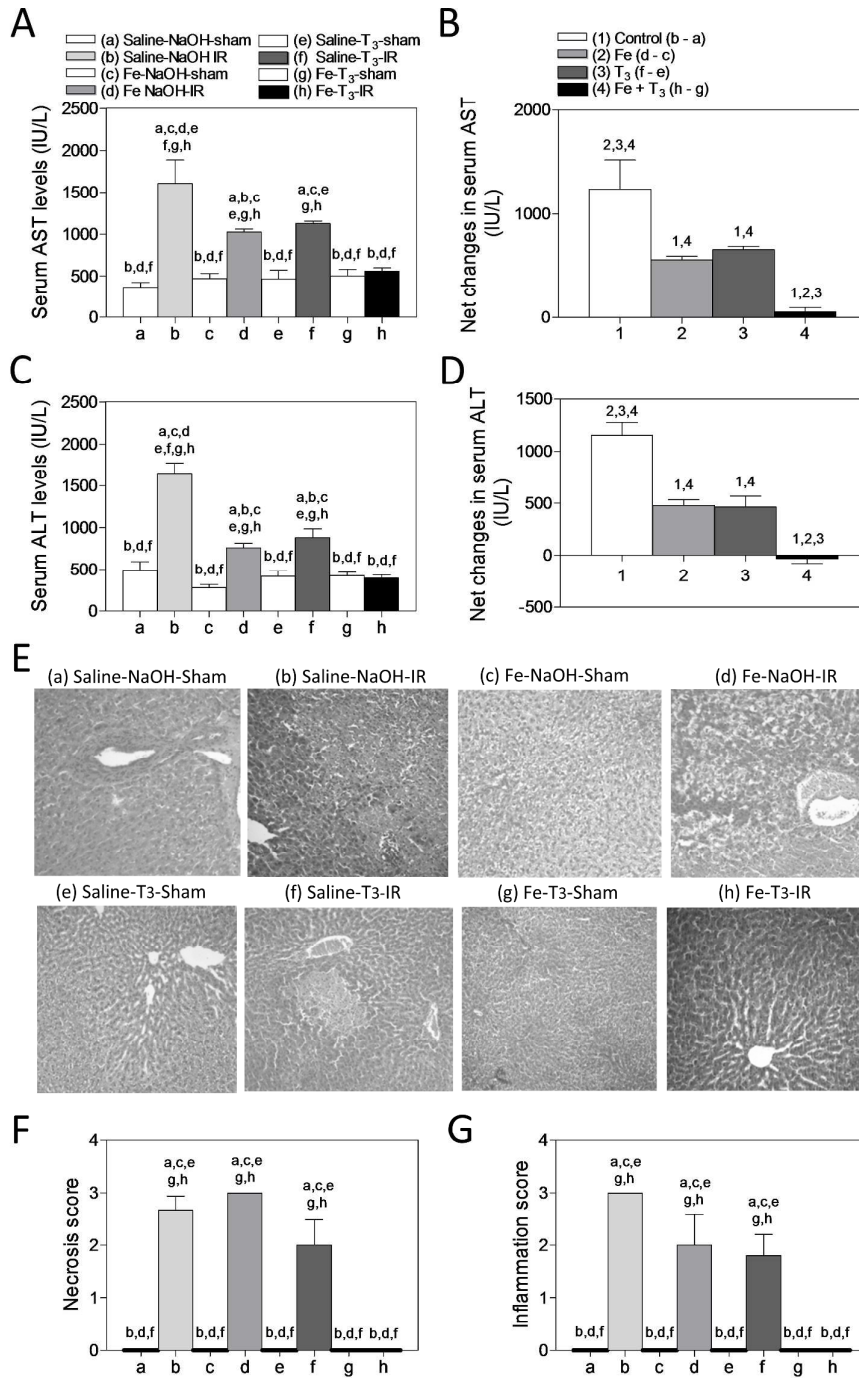


Figure 4

